Journal of Materials Chemistry C

ROYAL SOCIETY OF CHEMISTRY

PAPER

View Article Online
View Journal | View Issue

Cite this: J. Mater. Chem. C, 2022, 10, 4955

A phosphorescent OLED with an efficiency roll-off lower than 1% at 10 000 cd m^{-2} achieved by reducing the carrier mobility of the donors in an exciplex co-host system†

Chun-Hao Chiu,[a] Nurul Ridho Al Amin,[bcd] Jia-Xun Xie,[a] Chih-Chien Lee,[d] Dian Luo,[c] Sajal Biring,[bc] Kevin Sutanto,[bc] Shun-Wei Liu *[bc] and Chih-Hsin Chen *[a]

Received 18th September 2021,
Accepted 8th March 2022

DOI: 10.1039/d1tc04473g

rsc.li/materials-c

9,9′-Diphenyl-9*H*,9′*H*-3,3′-bicarbazole (BCzPh)-based molecules have been applied as donors in an exciplex co-host system in OLEDs to achieve high device performance. In this work, to investigate the effect of charge mobility of the donor on the performance of OLEDs using an exciplex co-host system, we synthesized two bipolar BCzPh analogs, *i.e.*, BCzPh-pimi and BCzPh-mimi, by introducing 1-phenyl-1*H*-benzimidazole to the *para*- and *meta*-positions of the phenyl ring of BCzPh. The ΔE_{ST} values of BCzPh-pimi and BCzPh-mimi are 0.60 eV and 0.59 eV, respectively. In contrast, the ΔE_{ST} values of the exciplex formed by BCzPh-pimi and BCzPh-mimi with an electron acceptor, *i.e.*, B3PyMPM, are 0.26 eV and 0.19 eV, respectively. In addition, the photoluminescence (PL) decay lifetimes of BCzPh-pimi and BCzPh-mimi increase remarkably from 5.39 ns and 9.46 ns to 247.79 ns and 263.21 ns, respectively, when mixed with B3PyMPM. The OLEDs fabricated by using BCzPh-pimi with B3PyMPM as an exciplex co-host for a green phosphorescence emitter, *i.e.*, Ir(ppy)$_2$(acac), exhibited a maximum external quantum efficiency (EQE) of 22.31%. Notably, the BCzPh-pimi-based device showed an extremely low efficiency roll-off. Its EQE was retained at 22.16% even at a high luminance of 10 000 cd m^{-2}, corresponding to the efficiency roll-off of only 0.67%. Such an extremely low efficiency roll-off of the device can be attributed to the reduced hole mobility of BCzPh-pimi resulting from the electron-withdrawing benzimidazole moiety in the molecular structure of BCzPh, which improves balance in charge recombination in the exciplex co-host system of OLED devices at high applied voltages.

Introduction

Conventional studies on organic light-emitting diodes (OLEDs) aim to avoid the formation of exciplexes in the emitting layer (EML) because the molecular aggregation leads to emission quenching, shifting, and decrease in the external quantum efficiency (EQE) of the devices. In 2012, Adachi's group demonstrated that excitons at non-radiative triplet states can be converted to radiative singlet states *via* reverse intersystem crossing (RISC) in an exciplex formed by electron-donating and electron-accepting molecules as the emitters of OLEDs.[1,2] This finding breaks the limitation of the internal quantum efficiencies of the OLEDs using fluorescent emitters due to the creation of non-radiative triplet excited states. Since then, the applications of exciplex systems to achieve high device performance attracted much attention in recent OLED studies. The formation of an exciplex generates new energy levels called "charge transfer (CT) energy levels", which offer an extremely small energy gap between the singlet and triplet excited states and therefore facilitate the RISC process of the emitters and promote the higher performance of OLED devices.[3,4]

By taking advantage of harvesting the triplet excitons through RISC, the exciplex formed by electron-donating and electron-accepting molecules was also applied as the host in OLEDs recently.[5–11] Compared to the unipolar host system, the exciplex-based bipolar co-host system is beneficial for the balance of charge carriers, as well as the broadening of the charge recombination zone in the EML of OLEDs.[12] These characteristics are beneficial for reducing the efficiency

[a] Department of Chemistry, Tamkang University, New Taipei 251, Taiwan. E-mail: chc@mail.tku.edu.tw
[b] Organic Electronics Research Center, Ming Chi University of Technology, New Taipei 24301, Taiwan. E-mail: swliu@mail.mcut.edu.tw
[c] Department of Electronic Engineering, Ming Chi University of Technology, New Taipei 24301, Taiwan
[d] Department of Electronic Engineering, National Taiwan University of Science and Technology, Taipei 10617, Taiwan

† Electronic supplementary information (ESI) available. See DOI: 10.1039/d1tc04473g

roll-offs of OLEDs. For example, Kim's group reported an OLED device using mCBP:PO-T2T as the exciplex-based bipolar co-host and FIrpic as the phosphorescent guest emitter with a maximum EQE of 34.1%, which is much higher than that of the device using mCBP as the unipolar host and FIrpic as the phosphorescent guest emitter, *i.e.*, 19.0%.[13,14] These results demonstrated that using an exciplex-based bipolar host is an ideal strategy to improve the device performance of OLEDs.

In recent years, the development of OLED technologies was not only focused on the applications in displays but also their applications in lighting, which requires the OLEDs to retain high device performance at high luminance values (>5000 cd m^{-2}).[15] The main reason for the efficiency roll-off at high luminance is the unbalanced recombination of charge carriers in the EML of OLEDs with an increase in voltage. In such circumstances, the difference in charge mobility for hole- and electron-transporting layers is amplified, which results in a decrease in the number of excitons recombining in the EML as well as the device performance. Finding out the two different organic molecules possessing identical hole- and electron-transporting mobility is too difficult to fulfill, as the mobility of most hole-transporting materials is at least one order of magnitude larger than that of electron-transporting materials. Due to the bipolar feature of the exciplex co-host, the strategies for using them to achieve low efficiency roll-offs of OLEDs are extremely valuable to be investigated. For instance, Lin *et al.* reported a strategy to reduce the efficiency roll-off by using an interfacial exciplex host for a TADF emitter. The highest EQE of their device reached 14.9% with a low efficiency roll-off of 4.0% at 1000 cd m^{-2}. However, the roll-off of this device increased sharply to 38.2% at 10 000 cd m^{-2}.[16] Later on, Chen *et al.* reported phosphorescent OLEDs with an extremely low efficiency roll-off by using acridine-based donors in the exciplex co-host system. When $Ir(ppy)_2(acac)$ was used as the emitter, the highest EQE of the device reached 14.7%, with the efficiency roll-offs of 1.4% and 4.1% at 5000 cd m^{-2} and 10 000 cd m^{-2}, respectively.[17] Based on previous findings, it is believed that well-balanced mobility in the EML is critical for governing the efficiency roll-offs of exciplex-based OLEDs. Nevertheless, the studies on balancing the charge mobility for an exciplex co-host system are still rare, especially for the devices that achieve extremely low efficiency roll-offs at luminance values larger than 10 000 cd m^{-2}.

In previous studies, phenylcarbazole-based molecules, such as 9,9-diphenyl-9*H*, 9′*H*-3,3-bicarbazole (BCzPh), have been applied as donor molecules in exciplex co-host systems for phosphorescent emitters to achieve high efficiency due to their high triplet energy. For example, Shih *et al.* reported an efficient exciplex co-host system using BCzPh as the donor and 2,4,6-tris(2-(1*H*-pyrazol-1-yl)phenyl)-1,3,5-triazine (3P-T2T) as the acceptor, which was doped with $Ir(ppy)_2(acac)$ as the emitter to fabricate phosphorescent OLEDs with an EQE of 29.7% and a low efficiency roll-off of 8.1% at 10 000 cd m^{-2}.[18] More recently, our group investigated the effect of the molecular structures of BCzPh-based donors in an exciplex co-host system on the EQE of OLEDs. The EQE of the phosphorescent OLEDs using $Ir(ppy)_2(acac)$ as the emitter could reach 31.5% with an efficiency roll-off of 18.6% at 10 000 cd m^{-2} by increasing the intermolecular distance between the donor and the acceptor in an exciplex co-host system.[19] This result demonstrated that the performance of the OLEDs using exciplex co-host systems is significantly affected by the molecular structure of the donor used to form the exciplex. Nevertheless, the structural effect of the BCzPh-based donors on their charge mobility, and how the mobility of the BCzPh-based donors affects the efficiency roll-off of the OLEDs using exciplex co-host systems have never been investigated before.

In this work, we synthesized two BCzPh analogs, namely BCzPh-pimi and BCzPh-mimi, by connecting BCzPh with an electron-withdrawing benzimidazole moiety at the *para*- and *meta*-positions of the phenyl ring on BCzPh. These two molecules were applied as the donor together with 4,6-bis(3,5-di(pyridin-3-yl)phenyl)-2-methylpyrimidine (B3PyMPM) as the acceptor to form an exciplex co-host system for OLEDs. According to previous reports, the hole mobility of BCzPh (1.13×10^{-5} cm^2 V^{-1} s^{-1}) was reported to be higher than the electron mobility of B3PyMPM (7.79×10^{-6} cm^2 V^{-1} s^{-1}). It is anticipated that the charge mobility of BCzPh-based molecules can be reduced by introducing an electron-withdrawing benzimidazole moiety on the molecular structure of BCzPh, which will be beneficial for the charge balance in exciplex-based co-host systems and the corresponding efficiency roll-offs of OLEDs. The fluorescence spectra, phosphorescence spectra and photoluminescence (PL) decay lifetimes of the exciplex of BCzPh-pimi/B3PyMPM and BCzPh-mimi/B3PyMPM in film states were recorded to evaluate the charge transfer characteristics of exciplex-based co-host systems. In addition, the hole mobilities of BCzPh-pimi and BCzPh-mimi were measured to study the effect of the molecular structures on the carrier mobilities of BCzPh-based molecules. Finally, the electrical properties of the OLEDs using a co-host system of the exciplex of BCzPh-pimi/B3PyMPM and BCzPh-mimi/B3PyMPM were investigated. These data were combined to investigate the effect of carrier mobility of the donor in an exciplex co-host system on the efficiency roll-offs of OLEDs.

Experimental section

Materials and methods

All chemicals used in the experiment were purchased from Sigma, Aldrich, Acros, TCI, Riedel-de Haen, J. T. Baker, Merck, Macron, Combi-Block, Aencore and Fluka. THF and toluene were dried *via* a solvent purification system when the reaction proceeded under moisture-free conditions. All reactions were executed under a nitrogen atmosphere and removed the solvents using a vacuum line and Schlenk line. Crude products were tracked by thin-layer chromatography (TLC) and purified by silica gel column chromatography (60–200 mesh, SiliCycle Inc.). Absorption spectra were recorded using a Thermo Scientific Evolution 60s UV-Vis spectrophotometer by dissolving the sample in toluene with a concentration of 10^{-5} M. In addition,

fluorescence spectra were recorded using an F-2500 Hitachi fluorescence spectrometer by dissolving the sample in toluene with a concentration of 10^{-5} M. ^{1}H and ^{13}C NMR spectra were recorded using a Bruker AC-300 FT-NMR/AC-600 FT-NMR spectrometer (300 MHz and 600 MHz) with a sample dissolved in $CDCl_3$. Mass spectra were recorded using a JEOL JMS-700 system, Tokyo, Japan, usually alternating fast atom bombardment (FAB) and electron ionization (EI) as an ionization source. The measurements of thermogravimetric analysis (TGA) were carried out using a PerkinElmer Pyris 1 TGA instrument with a heating rate of 10 °C min^{-1} under a nitrogen atmosphere. The measurements of differential scanning calorimetry (DSC) were carried out on a PerkinElmer Pyris 1 DSC with a heating rate of 8 °C min^{-1} and a cooling rate of 8 °C min^{-1} under nitrogen. All measurements of the redox reaction were performed using a 10^{-3} M sample mixed with a 0.1 M supporting electrolyte (tetrabutylammonium hexafluorophosphate, $TBAPF_6$) in dichloromethane and purged with nitrogen for 10 min. The prepared sample was estimated using a three-electrode system composed of Ag/AgCl as the reference electrode, platinum as the counter electrode and glassy-carbon as the working electrode. According to UV-vis and PL spectra, the energy gaps of samples were obtained. After the oxidation potentials (E_{ox}) were estimated, the HOMO of the samples was gained using ferrocene (Fc) as an external standard. Eventually, the LUMO of the samples were gained by adding the HOMO and E_g values.

Synthetic procedure and characterization of BCzPh-pimi and BCzPh-mimi

9-Phenyl-9*H*,9′*H*-3,3′-bicarbazole was prepared using 2-(3-bromophenyl)-1-phenyl-1*H*-benzo[*d*]imidazole and 2-(4-bromophenyl)-1-phenyl-1*H*-benzo[*d*]imidazole *via* a Ullmann reaction. Both acceptors were synthesized by primitive procedures. Compounds BCzPh-pimi and BCzPh-mimi were synthesized under similar conditions. Consequently, only BCzPh-pimi would be discussed in detail.

Synthesis of 9-phenyl-9′-(4-(1-phenyl-1*H*-benzo[*d*]imidazol-2-yl)phenyl)-9*H*,9′H-3,3′-bicarbazole (BCzPh-pimi). Under a nitrogen atmosphere, a mixture of 9-phenyl-9*H*,9′*H*-3,3′-bicarbazole (1180 mg, 2.88 mmol), 2-(4-bromophenyl)-1-phenyl-1*H*-benzo[*d*]imidazole (2787 mg, 7.98 mmol), copper(I) iodide (124 mg, 0.65 mmol), anhydrous potassium carbonate (795 mg, 5.75 mmol), 18-crown-6 (14 mg, 0.056 mmol) and 1,3-dimethyl-3,4,5,6-tetrahydro-2(1*H*)-pyrimidinone (DMPU, 20 mL) was heated to 170 °C for 24 h. After cooling to room temperature, the crude product was filtered through celite to remove the remaining copper. The reaction mixture was quenched by the addition of water and extracted with dichloromethane, and the water was removed by adding anhydrous Mg_2SO_4. Eventually, the crude product was purified by silica gel column chromatography with ethyl acetate/hexane (1 : 8 by volume) as the eluent, and then recrystallized with methanol and THF. The purified product was obtained as a white solid (1413 mg, yield of 72.3%). ^{1}H NMR (600 MHz, $CDCl_3$): δ (ppm) = 8.454–8.439 (d, J = 3.9, 2H), 8.247–8.22 (t, 2H), 7.955 (d, J = 4.2, 1H), 7.866–7.852 (d, J = 4.2, 2H), 7.791–7.76 (t, 2H), 7.641–7.569 (m, 8H), 7.557–7.495 (m, 4H), 7.461–7.422 (m, 6H), 7.408–7.381 (t, 1H), 7.338–7.294 (m, 4H). ^{13}C NMR (75 MHz, $CDCl_3$): δ (ppm) = 142.98, 141.32, 140.81, 140.02, 139.48, 138.82, 137.72, 137.35, 136.90, 134.69, 134.13, 130.84, 130.03, 129.85, 128.85, 128.67, 127.48, 127.40, 127.01, 126.40, 126.13, 126.03, 125.87, 125.72, 124.21, 123.95, 123.81, 123.57, 123.51, 123.17, 120.44, 120.34, 119.96, 119.90, 118.85, 118.82, 110.51, 109.98, 109.85. *m*/*z*: $[M + H]^+$ calcd for $C_{49}H_{32}N_4$, 677.2705; found, 677.2695.

Synthesis of 9-phenyl-9′-(3-(1-phenyl-1*H*-benzo[*d*]imidazol-2-yl)phenyl)-9*H*,9′*H*-3,3′-bicarbazole (BCzPh-mimi). BCzPh-mimi was obtained as a pale white powder (500 mg, yield of 25.6%). ^{1}H NMR (600 MHz, $CDCl_3$): δ (ppm) = 8.439 (d, J = 1.2 Hz, 1H), 8.395 (d, J = 1.2 Hz, 1H), 8.25–8.24 (d, J = 7.8 Hz, 1H), 8.18–8.17 (d, J = 7.2 Hz, 1H), 7.76–7.74 (m, 1H), 7.68–7.61 (m, 13H), 7.52–7.51 (m, 1H), 7.45–7.42 (m, 5H), 7.33–7.28 (m, 7H), 7.12 (d, J = 8.4, 1H), 7.04 (d, J = 8.4 Hz, 1H). ^{13}C NMR (75 MHz, $CDCl_3$): δ (ppm) = 142.96, 141.32, 140.90, 140.02, 139.58, 137.73, 137.64, 137.31, 136.81, 134.51, 134.25, 132.02, 130.26, 130.23, 129.86, 128.72, 128.46, 127.77, 127.51, 127.41, 127.02, 126.06, 126.04, 125.83, 125.77, 123.99, 123.94, 123.67, 123.57, 123.51, 123.21, 120.37, 120.28, 120.12, 120.01, 119.97, 118.83, 118.77, 110.53, 109.99, 109.86, 109.77, 109.64. *m*/*z*: $[M]^+$ calcd for $C_{49}H_{32}N_4$, 676.2627; found, 676.2621.

OLED device fabrication and characterization

OLED devices were fabricated onto a sputtered indium-tin-oxide (ITO) coated glass substrate, which was prepared in our lab using a sputtering machine system. The glass substrate was cleaned carefully before the ITO was deposited at around 80 nm thickness onto the clean glass surface. The glass substrate was sequentially soaked in DI (deionized) water, acetone and IPA (isopropyl alcohol) solution under ultrasonic vibration for 10 minutes, and dried using a nitrogen (N_2) blower. The organic and inorganic materials used for the device fabrication are as follows: HATCN (1,4,5,8,9,11-hexaazatriphenylene hexacarbonitrile), TAPC (4,4′-cyclohexylidenebis[*N*,*N*-bis(4-methylphenyl)-benzenamine]), Ir(ppy)$_2$(acac) (bis[2-(2-pyridinyl-*N*)phenyl-*C*]-(acetylacetonato)iridium(III)), B3PyMPM (4,6-bis(3,5-di(pyridin-3-yl)phenyl)-2-methylpyrimidine), LiF (lithium fluoride), and Al (aluminum). All the organic and inorganic materials used for the device fabrication were purchased from Shine Material Technology Co., Ltd. Furthermore, the organic materials were purified using a homemade purification system in our laboratory at a vacuum level of $\sim 5 \times 10^{-6}$ Torr. OLED devices were fabricated using an ITO coated glass substrate in a thermal evaporation system at a vacuum level of $\sim 2 \times 10^{-6}$ torr. The organic materials and aluminum were deposited at constant deposition rates of 0.5–1 Å s^{-1} and 5 Å s^{-1}, respectively. All the deposited material thicknesses were monitored using quartz crystal measurement. For the final process, the OLED device was encapsulated using encapsulation glass inside a glovebox under moisture (H_2O) and oxygen (O_2) conditions of <0.1 ppm.

Furthermore, to understand the device characterization and performance, the current density–voltage–luminance characteristics (*J*–*V*–*L*), current and power efficiency at different luminance values, external quantum efficiency (EQE) and device

spectral emission of the OLED device were measured using an integrated sphere machine from Enlitech (Enli Tech LQ-100x series) connected to a source/measure unit (Keysight B2901A). All the data were obtained using built-in software from Enlitech.

The hole and electron charge mobilities of each material were determined using SCLC measurement, which was carried out using a Keithley 2400 source meter. The material thin-film was deposited onto an ITO glass substrate with a thickness of around 200 nm. The hole and electron mobilities of each material were characterized using the Mott–Gurney equation, as shown below

$$J = \frac{9}{8}\varepsilon\varepsilon_0\mu\frac{V^2}{d^3}$$

where J is the current density, ε and ε_0 are the relative permittivity and permittivity of vacuum, V is the applied bias voltage, and d is the thin-film thickness.

Photophysical characterization

The photophysical characteristics of the material such as steady-state emission spectra and time-resolved photoluminescence (TRPL) were measured in a nitrogen-filled chamber using a spectrofluorometer (HORIBA Scientific FluoroMax Plus). The steady-state emission spectra measurement of each thin-film sample was done using excitation light (ozone-free xenon arc lamp) under excitation at 305 nm. The TRPL measurement was done using a NanoLED pulse diode controlled as excitation light (N-320, HORIBA Jobin Yvon) under excitation at 320 nm with an excitation frequency of 250 kHz.

Theoretical calculation

All simulated results were calculated using the Gaussian 09 software. All theoretical calculations were performed using the Gaussian 09 software. The geometric optimization calculations of the molecular structures were performed using density functional theory (DFT) at B3LYP/6-31G(d) levels for both bipolar compounds.

Results and discussion

Synthesis and characterization of BCzPh-pimi and BCzPh-mimi

Scheme 1 shows the molecular structures and synthetic routes of BPhCz-pimi, BPhCz-mimi. They were obtained by Ullmann coupling reactions between 9-phenyl-9*H*,9′*H*-3,3′-bicarbazole and 2-(4-bromophenyl)-1-phenyl-1*H*-benzimidazole or 2-(4-bromophenyl)-1-phenyl-1*H*-benzimidazole. The details of the synthetic conditions of BPhCz-pimi and BPhCz-mimi referred to the previous studies and can be found in the experimental section.[20–22] BCzPh-pimi and BCzPh-mimi can be readily dissolved in dichloromethane, chloroform, and toluene. Consequently, they were purified by column chromatography and identified by ^{1}H NMR spectroscopy, ^{13}C NMR spectroscopy, and high-resolution mass spectrometry.

Theoretical calculation

Next, density functional theory (DFT) calculations were performed to simulate the spatial distribution of molecular orbitals and the optimized molecular geometry and electronic distribution of BCzPh-pimi and BCzPh-mimi. As depicted in Fig. 1, the highest occupied molecular orbitals (HOMOs) of BCzPh-pimi and BCzPh-mimi are primarily located at the moiety of the electron-donating group, *i.e.*, diphenyl bicarbazole. On the other hand, the lowest unoccupied molecular orbitals (LUMOs) of BCzPh-pimi and BCzPh-mimi are primarily located at the moiety of the electron-withdrawing group, *i.e.*, benzimidazole, and the phenyl ring between the bicarbazole moiety and the benzimidazole moiety. The overlapping of the HOMOs and LUMOs ensures the charge-transfer characteristics of BCzPh-pimi and BCzPh-mimi. From their optimized molecular geometries, it was found that the

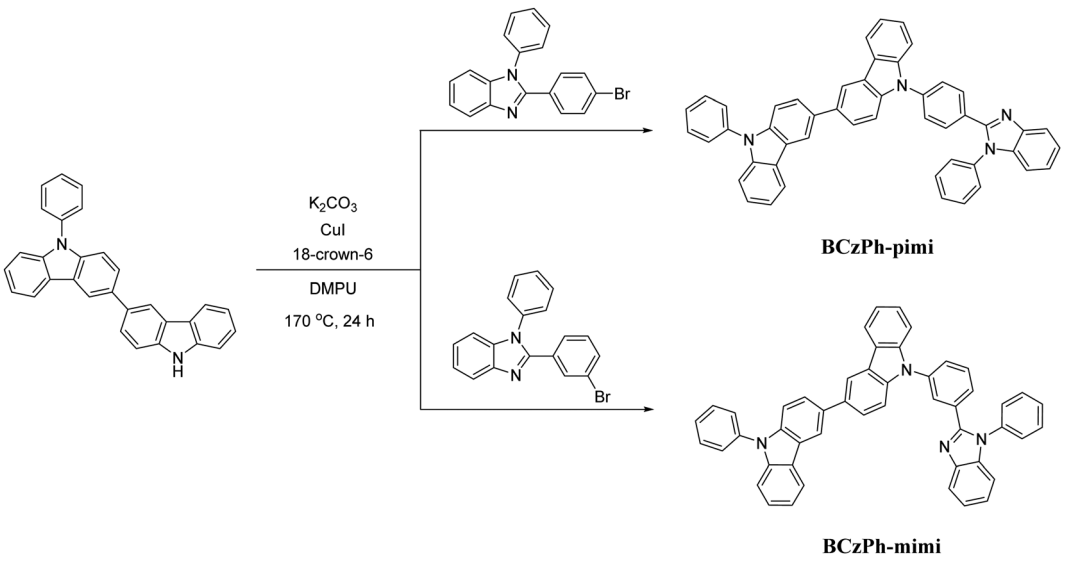

Scheme 1 Synthetic routes of BCzPh-pimi and BCzPh-mimi.

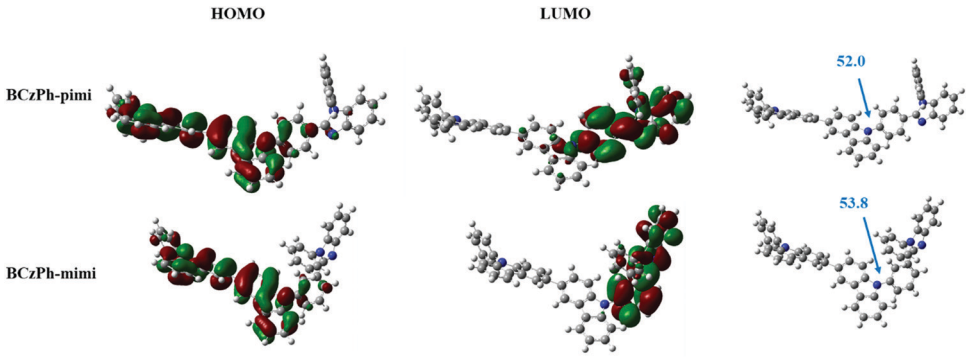

Fig. 1 Molecular orbital distributions and molecular geometries of BCzPh-pimi and BCzPh-mimi.

dihedral angle between the carbazole and the phenyl ring attached to benzimidazole for BCzPh-pimi and BCzPh-mimi are 52.0° and 53.8°, respectively, suggesting the nonplanar structure of these molecules. The smaller dihedral angle of BCzPh-pimi also explains why its LUMO extends to the nitrogen atom of the carbazole moiety, while this phenomenon was not observed for the LUMO of BCzPh-mimi.

Thermal properties

The thermal properties of BCzPh-pimi and BCzPh-mimi were studied by thermogravimetric analysis (TGA) and differential scanning calorimetry (DSC) because the thermal-decomposition temperature (T_d) and the glass transition temperatures (T_g) of the host molecules are significant factors affecting the performance and lifetime of their corresponding OLED devices. As shown in Fig. S1 (ESI†) and Table 1, the T_ds (corresponding to 5% weight loss) of BCzPh-pimi and BCzPh-mimi are 416.6 °C and 324.8 °C, respectively. The higher T_d value of BCzPh-pimi can be explained by the structural rigidity when the benzimidazole moiety was *para*-substituted on the phenyl ring of diphenyl bicarbazole. A similar trend was observed for the T_gs of BCzPh-pimi and BCzPh-mimi. The T_g value of BCzPh-pimi, *i.e.*, 145.7 °C, is much higher than that of BCzPh-mimi, *i.e.*, 104.8 °C, which can be attributed to the larger spatial molecular structure of BCzPh-mimi.

Photophysical and electrochemical properties

The UV-Vis absorption spectra and photoluminescence (PL) spectra of BCzPh-pimi and BCzPh-mimi were recorded to investigate how the molecular structure affects their photophysical properties. The detailed data are presented in Table 1. As shown in Fig. 2a, the main absorption bands of BCzPh-pimi and BCzPh-mimi are similar, which are located at 303 nm and 304 nm, respectively. These absorption bands are also similar to that of the bicarbazole moiety measured under the same conditions (Fig. S2, ESI†), so it can be attributed to the localized π–π* transitions of the bicarbazole moiety. In addition, a shoulder band located at 338 nm was observed in the absorption spectra of BCzPh-pimi and BCzPh-mimi. According to the previous report, BCzPh exhibits a main absorption band at 303 nm, which is similar to those of BCzPh-pimi and BCzPh-mimi.[23] However, no shoulder band was observed for BCzPh. Therefore, the shoulder band located at 338 nm can be attributed to the weak charge-transfer from the bicarbazole moiety and the benzimidazole moiety of the molecule, which is in accordance with the phenomenon we found in theoretical calculation. In terms of the PL spectra, a solvatochromic study revealed that BCzPh-pimi and BCzPh-mimi exhibit emission bands at 403 nm and 404 nm in toluene, respectively, while this band was red-shifted in more polar solvents, *i.e.*, dichloromethane, DMF and acetonitrile (Fig. S3, ESI†). This phenomenon further identified the charge-transfer characteristics of these molecules at their excited state. From the optical onset of their absorption bands, the energy gaps of BCzPh-pimi and BCzPh-mimi were calculated to be 3.33 eV and 3.47 eV, respectively. In contrast, the energy gap of BCzPh was reported to be 3.37 eV in a previous report, which is larger than that of BCzPh-pimi. These results suggest that BCzPh-pimi possesses a more effective π-conjugation length than BCzPh-mimi and BCzPh.

To investigate the energy levels of the molecular orbitals, the electrochemical properties of BCzPh-pimi and BCzPh-mimi were measured by cyclic voltammetry (CV). As illustrated in Fig. 2b, BCzPh-pimi and BCzPh-mimi exhibited two quasi-reversible redox waves attributed to the two carbazole moieties. Combining the oxidative potentials of the molecules obtained by CV and the optical onset of their absorption bands obtained

Table 1 Photophysical, thermal and electrochemical properties of BCzPh-pimi and BCzPh-mimi

Exciplex donor	T_g/T_d [°C]	λ_{abs}[a] [nm]	λ_{em}[a] [nm]	λ_{phos}[b] [nm]	HOMO/LUMO [eV]	E_g [eV]	S_1 [eV]	T_1 [eV]	ΔE_{ST} [eV]
BCzPh-pimi	145.7/416.6	303, 338	405	529	−5.41/−2.08[c], −4.99/−1.26[d]	3.33[c], 3.73[d]	3.23	2.63	0.60
BCzPh-mimi	104.8/324.8	304	405	535	−5.35/−1.89[c], −5.01/−1.24[d]	3.46[c], 3.77[d]	3.30	2.71	0.59

[a] Measured in toluene with 10^{--5} M at room temperature. [b] Measured as films at 77 K. [c] Experimental values measured by cyclic voltammetry and calculated using absorption bands. [d] Theoretical values calculated using the Gaussian 09 software.

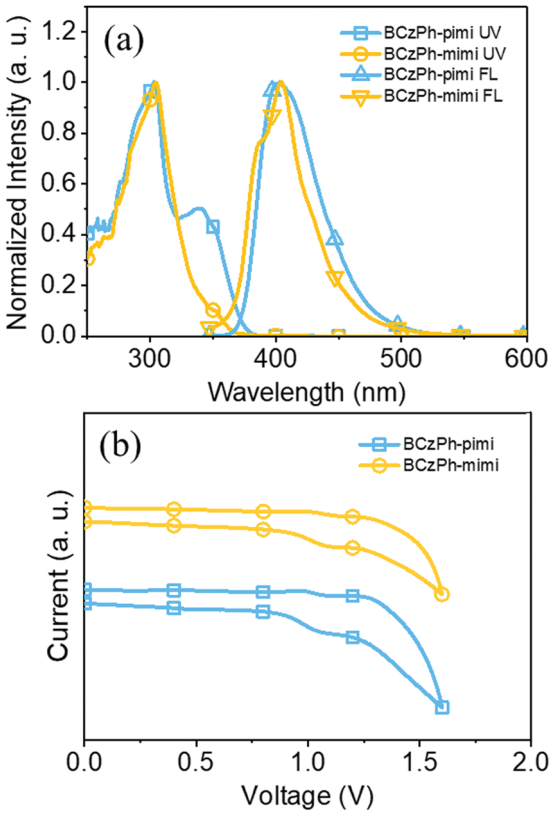

Fig. 2 (a) UV-Vis and fluorescence spectra and (b) cyclic voltammograms of BCzPh-pimi and BCzPh-mimi in toluene.

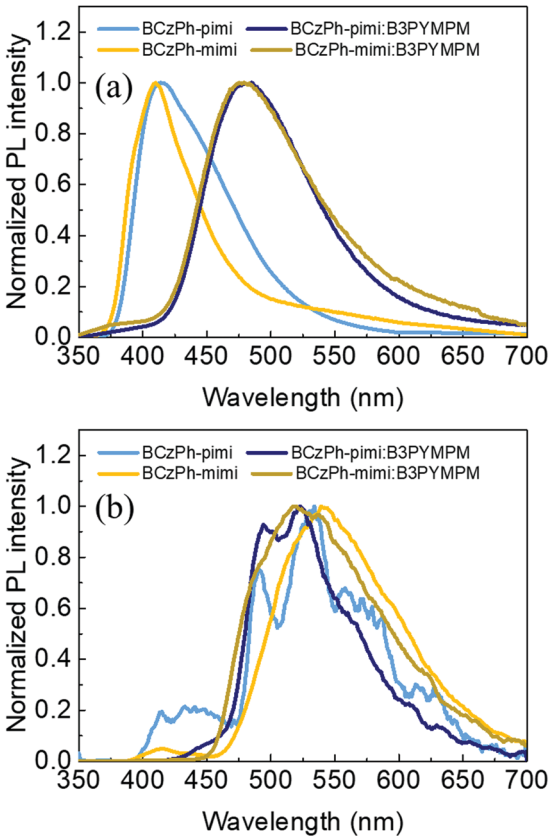

Fig. 3 Photoluminescence spectra of the bare films of BCzPh-pimi and BCzPh-mimi and their blended films with B3PyMPM recorded at (a) room temperature and (b) 77 K (excitation: 325 nm).

by UV-Vis spectra, the HOMO/LUMO energy levels of BCzPh-pimi and BCzPh-mimi were calculated to be −5.41/−2.08 eV and −5.35/−1.89 eV, corresponding to the energy gaps of 3.33 eV and 3.47 eV, respectively. The calculated HOMO/LUMO energy levels of BCzPh-pimi and BCzPh-mimi are −4.99/−1.26 eV and −5.01/−1.24 eV, corresponding to the energy gaps of 3.73 eV and 3.77 eV, respectively. The smaller energy gap of BCzPh-pimi can be explained by its more effective π-conjugation system such that the electronic interaction between bicarbazole and benzimidazole moieties is stronger. The above results, when combined, led us to conclude that the electron-donating ability of BCzPh can be reduced by introducing a benzimidazole moiety into its molecular structure. This effect is more dominant when benzimidazole was linked to the *para*-position of the phenyl of BCzPh.

Photophysical analysis of the exciplex formation

To evaluate the suitability of BCzPh-pimi and BCzPh-mimi to be applied as a donor in the exciplex host system, the steady-state photoluminescence spectra of the bare films of BCzPh-pimi and BCzPh-mimi, as well as the blended films of BCzPh-pimi and BCzPh-mimi/B3PyMPM (1 : 1 molar ratio), were recorded. Fig. 3a shows that the emission peaks of the bare films of BCzPh-pimi and BCzPh-mimi at room temperature are located at 414 nm and 410 nm, respectively. In contrast, the films of both BCzPh-pimi and BCzPh-mimi blended with B3PyMPM exhibit more red-shifted emission peaks at 485 nm and 479 nm, respectively. In addition, we noted that the profile of the emission spectrum of the blended films was quite different from that of bare films. These results can be explained by the formation of a new charge transfer (CT) state in the blended films of BCzPh-pimi and BCzPh-mimi/B3PyMPM, suggesting the exciplex formation in this system. On the other hand, the blended film of BCzPh-pimi and B3PyMPM exhibited an absorption peak at around 300 nm attributed to B3PyMPM, and an absorption peak at around 350 nm attributed to BCzPh-pimi. In addition, the blended films showed a slightly blue-shifted absorption band compared to that of BCzPh-pimi, suggesting that a weak electronic interaction exists between the donor and the acceptor in the ground state of the exciplex. (Fig. S4, ESI†). Furthermore, the singlet and triplet energies of the blended films of BCzPh-pimi and BCzPh-mimi/B3PyMPM were calculated from their photoluminescence spectra at room temperature and 77 K (Fig. 3a and b), and the detailed data are included in Table 2. The singlet–triplet energy gaps (ΔE_{ST}s) of BCzPh-pimi/B3PyMPM and BCzPh-mimi/B3PyMPM films are 0.26 eV and 0.19 eV, respectively.

Device performance and efficiency roll-off

To investigate the electroluminescence (EL) behaviors of BCzPh-pimi and BCzPh-mimi as the donor in the exciplex

Table 2 Photophysical properties of BCzPh-pimi/B3PyMPM and BCzPh-mimi/B3PyMPM blended films

Exciplex co-host	λ_{em}[a] [nm]	λ_{phos}[a] [nm]	S_1 [eV]	T_1 [eV]	ΔE_{ST} [eV]
BCzPh-pimi/B3PyMPM	485	523	2.91	2.65	0.26
BCzPh-mimi/B3PyMPM	479	520	2.91	2.72	0.19

[a] Measured as films at room temperature.

co-host system, and how the molecular structure of the donor in the exciplex co-host system affects the performance of OLEDs, green OLED devices were fabricated using the device structure of ITO/HATCN (30 nm)/TAPC (30 nm)/BCzPh-pimi or BCzPh-mimi (15 nm)/BCzPh-pimi or BCzPh-mimi: B3PyMPM: 8 wt% $Ir(ppy)_2(acac)$ (30 nm; molar ratio of 1 : 1)/B3PyMPM (40 nm)/LiF (1 nm)/Al (120 nm). The energy diagrams and chemical structures of the materials applied in this device are shown in Fig. 4a. From the device structure, HATCN was used as the hole injection layer (HIL), TAPC and BCzPh-pimi or BCzPh-mimi as the hole transport layer (HTL), B3PyMPM as the electron transport layer (ETL), LiF as the electron injection layer (EIL), and ITO and Al were applied as the anode and cathode, respectively. $Ir(ppy)_2(acac)$ was applied as a green phosphorescent emitter. For the emission layer, the exciplex formation was utilized between BCzPh-pimi or BCzPh-mimi and B3PyMPM using a molar ratio of 1 : 1 to achieve efficient energy transfer. Among these devices, the BCzPh-pimi-based device is denoted as device P1, and the BCzPh-mimi-based device is denoted as device P2. For comparison, a reference device using BCzPh was fabricated. The EL characterization of the devices are shown in Fig. 4b–d, and the results are summarized in Table 3. The turn-on voltages at 100 cd m^{-2} for devices P1 and P2 were 2.9 V and 3.1 V, respectively, which were slightly higher than that of the reference device, *i.e.*, 2.6 V. The maximum EQE (η_{ext}), current efficiency (η_c) and power efficiency (η_p) were 22.31%, 84.11 cd A^{-1}, and 77.31 lm W^{-1} for device P1; 18.73%, 70.37 cd A^{-1},

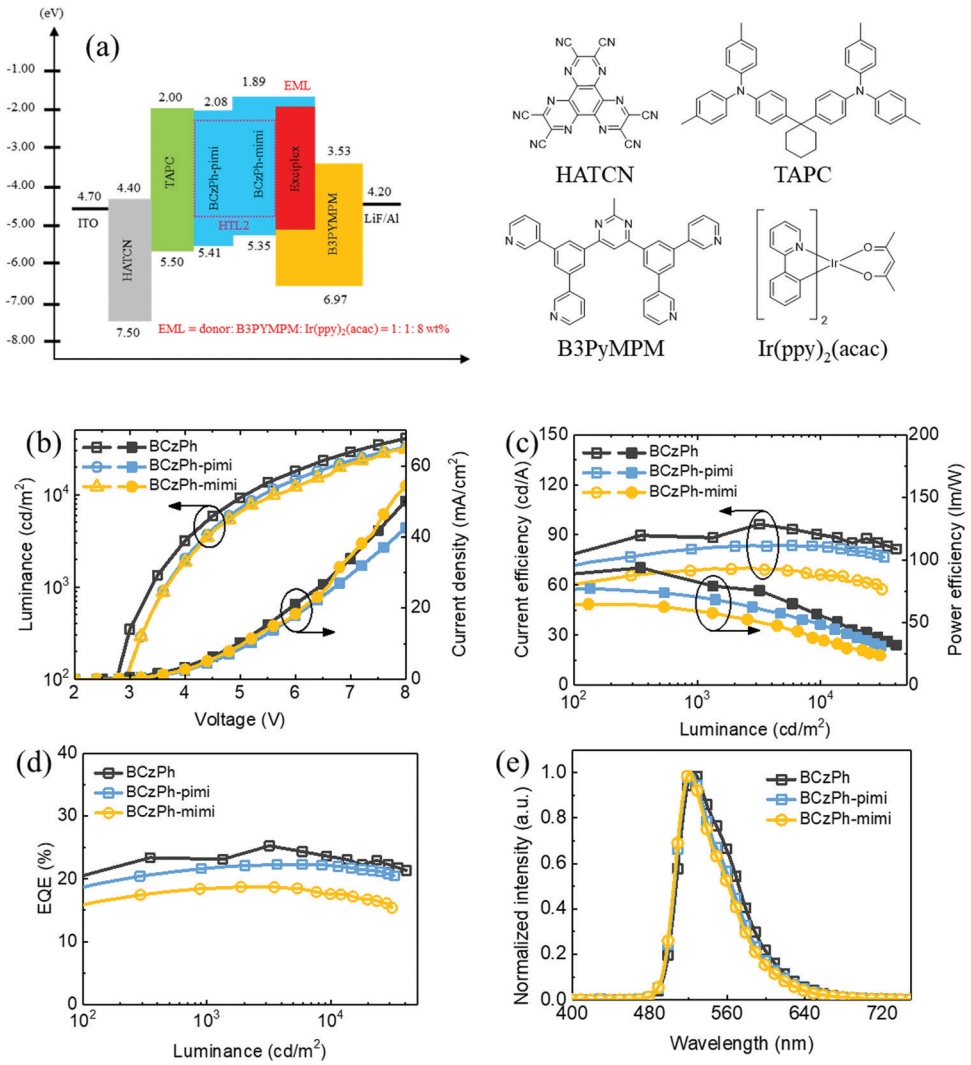

Fig. 4 (a) Energy level diagrams and molecular structures of devices, (b) current density–voltage–luminance (*J*–*V*–*L*) of devices with an exciplex as the host, (c) Current and power efficiency of devices with an exciplex as the host, (d) External quantum efficiency (EQE) *versus* luminance of devices with an exciplex as the host and (e) EL spectra of devices with an exciplex as the host, for PhOLEDs.

Table 3 Electroluminescence characteristics of green OLEDs using BCzPh-pimi, BCzPh-mimi and BCzPh as the donors in an exciplex co-host system

Device	Exciplex donor	V_{on}	η_c [cd A^{-1}] max., 1000, 10 000 cd m^{-2}	η_p [lm W^{-1}] max., 1000, 10 000 cd m^{-2}	η_{ext} [%] max., 1000, 10 000 cd m^{-2}	CIE [x, y]@max
P1	BCzPh-pimi	2.9	84.11, 81.83, 83.28	77.31, 70.64, 48.38	22.31, 21.70, 22.16	0.307, 0.644
P2	BCzPh-mimi	3.1	70.37, 68.98, 66.34	64.74, 59.33, 37.11	18.73, 18.46, 17.57	0.298, 0.649
Ref.	BCzPh	2.6	96.32, 88.83, 90.10	93.89, 84.34, 55.76	25.28, 23.22, 23.56	0.326, 0.634

and 64.74 lm W^{-1} for device P2; and 25.28%, 84.11 cd A^{-1}, and 77.31 lm W^{-1} for the reference device. The higher EQE of P1 can be explained by the higher photoluminescence quantum yield (PLQY) of the blended film of BCzPh-pimi and B3PyMPM, *i.e.*, 3.84%, than that of BCzPh-mimi and B3PyMPM, *i.e.*, 1.62%, which increased the efficiency of exciton capturing in the exciplex co-host system. In the EL characterization, Fig. 4e shows the normalized EL spectra for all devices with a peak at around 525 nm. These green EL emission spectra were compatible with the Ir-dopant emission without any additional peak exhibited in the emission spectrum. This result indicates that the efficient energy transfer from the host to the dopant was achieved because the emission inside the EML was completely from the phosphorescent dopant.

To verify the new charge transfer state in the exciplex forming system, the time-resolved photoluminescence (TRPL) measurement was performed and the corresponding data are presented in Table S1 (ESI†). TRPL measurement was used to show the decay profiles of the films of BCzPh-pimi and BCzPh-mimi materials, and the films of BCzPh-pimi or BCzPh-mimi blended with B3PyMPM. From Fig. 5a and b, it was found that BCzPh-pimi and BCzPh-mimi showed short prompt fluorescence emission, with lifetimes of 5.39 ns and 9.46 ns, respectively. In contrast, the blended films of BCzPh-pimi or BCzPh-mimi and B3PyMPM showed a shorter prompt emission with lifetimes of 63.73 ns and 54.16, respectively, while a longer fluorescence emission with lifetimes of 274.79 ns and 263.21 ns, respectively. The Lippert–Mataga plot obtained by solvatochromic experiments revealed that both BCzPh-pimi and BCzPh-mimi exhibited large dipole moments of 32.68 D and 33.73 D, respectively, in solvents of high polarity (see Fig. S5 and Tables S3, S4, ESI† for detailed calculations). Therefore, the elongated lifetime of the blended film could be attributed to the hybridized local and charge-transfer (HLCT) states formed in BCzPh-mimi and B3PyMPM.[24]

Finally, the efficiency roll-offs of the OLEDs were studied and compared with the reference device. The maximum EQEs of device P1, device P2 and reference device are 22.31%, 18.73%, and 25.54%, respectively. In terms of EQE, the efficiency roll-offs of device P1, device P2 and reference device at 1000 cd cm^{-2} are 2.73%, 1.44%, and 3.24%, respectively, whereas those at 10 000 cd cm^{-2} are 0.67%, 6.19%, and 6.61%, respectively. Apparently, the efficiency roll-offs of the devices using BCzPh-pimi and BCzPh-mimi were superior to that using BCzPh as the donor in the exciplex co-host system. In addition, it is worth mentioning that the efficiency roll-off of the BCzPh-pimi-based device was as low as 0.67% at 10 000 cd cm^{-2}. To the best of our knowledge, such an extremely low roll-off at high luminance for green OLEDs has never been reported in previous works. To further explore this phenomenon, the carrier mobility of each material applied in the exciplex co-host system was determined using SCLC measurement. The hole and electron mobilities were measured using the hole only device (HOD) structure of ITO/MoO_3 (5 nm)/BCzPh-pimi or BCzPh-mimi (200 nm)/MoO_3 (12 nm)/Ag (60 nm) for measuring the hole mobility and the electron only device (EOD) structure of ITO/BPhen:Cs_2Co_3 (5 nm, 15 wt%)/BCzPh-pimi or BCzPh-mimi (200 nm)/BPhen:Cs_2Co_3 (5 nm, 15 wt%)/Ag (60 nm) for measuring the electron mobility. For comparison, the hole mobility of the BCzPh material was measured using the HOD structure and the electron mobility of the B3PyMPM material was measured using the EOD structure. All the HOD and EOD structures were characterized using the SCLC Mott–Gurney method, where the results are depicted in Fig. 5c and d, and the mobility data are summarized in Table S2 (ESI†). The hole mobilities of BCzPh-pimi, BCzPh-mimi and BCzPh are 2.80×10^{-6} cm^2 V^{-1} s^{-1}, 1.13×10^{-6} cm^2 V^{-1} s^{-1}, and 1.13×10^{-5} cm^2 V^{-1} s^{-1}, respectively. It was found that the hole mobility of BCzPh was the highest among the three molecules, followed by BCzPh-pimi and BCzPh-mimi. As for B3PyMPM, the electron mobility was calculated to be 7.79×10^{-6} cm^2 V^{-1} s^{-1}. These results suggest that the hole mobility of BCzPh is lowered by introducing an electron-withdrawing benzimidazole moiety on the molecular structure of BCzPh. Considering the balance of carriers in the EML, the higher EQE of the reference device is attributed to the comparable carrier mobility of BCzPh and B3PyMPM. For the same reason, device P1 exhibited a higher EQE than device P2. On the other hand, the electron mobility was also measured to confirm the role of BCzPh-pimi and BCzPh-mimi in carrier transport in this system. Using the SCLC method, the electron mobilities of BCzPh-pimi and BCzPh-mimi were calculated to be 1.39×10^{-9} cm^2 V^{-1} s^{-1} and 5.98×10^{-9} cm^2 V^{-1} s^{-1}, respectively. This result implies that BCzPh-pimi and BCzPh-mimi could solely act as the hole transporting material in this system since their electron mobility was not satisfied to be a bipolar material. Furthermore, we performed SCLC analysis for the blend films to evaluate the carrier mobility of the blended films (Fig. S6 and Table S5, ESI†). The results showed that the hole and electron mobilities of the blended film of BCzPh-pimi and B3PyMPM were calculated as 2.79×10^{-9} cm^2 V^{-1} s^{-1} and 7.45×10^{-8} cm^2 V^{-1} s^{-1}, respectively. In contrast, the hole and electron mobilities of the blended film of BCzPh-mimi and B3PyMPM were calculated as 7.48×10^{-10} cm^2 V^{-1} s^{-1} and 2.67×10^{-10} cm^2 V^{-1} s^{-1}, respectively. The hole mobility of the blend films of BCzPh-pimi or BCzPh-mimi with B3PyMPM is more than three orders of magnitude lower than that of the

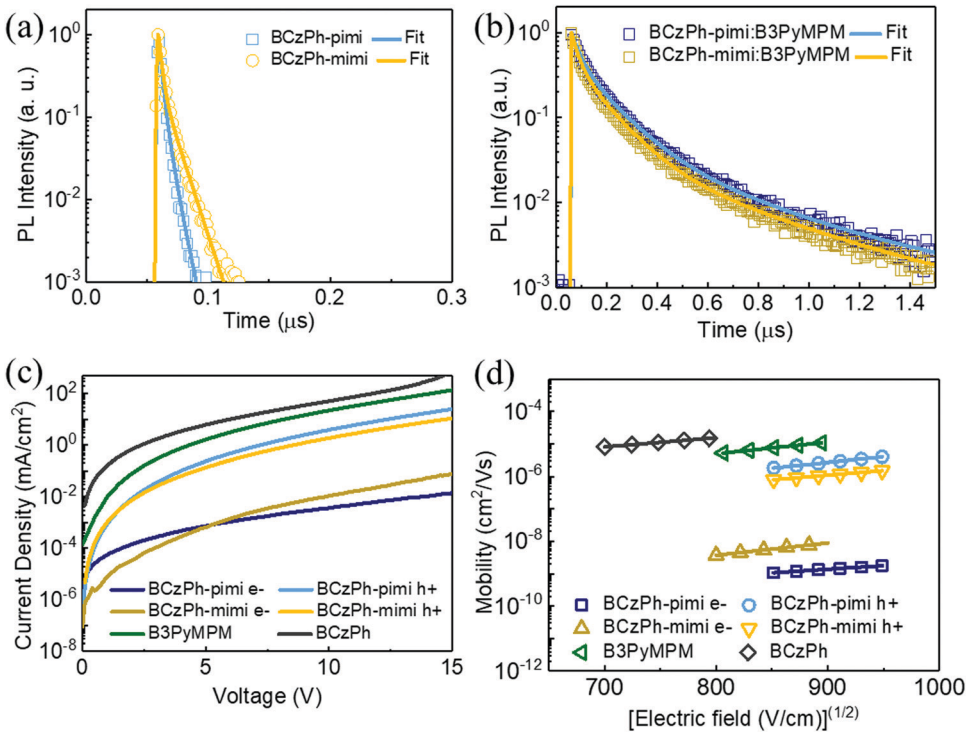

Fig. 5 (a) PL decay profiles of (a) bare BCzPh-pimi and BCzPh-mimi films and (b) BCzPh-pimi/B3PyMPM and BCzPh-mimi/B3PyMPM blended films. (c) Current densities of hole and electron only devices. (d) Hole and electron mobilities of each material.

bare films of BCzPh-pimi or BCzPh-mimi, while the electron mobility of the blend films of BCzPh-pimi or BCzPh-mimi with B3PyMPM is more than two orders of magnitude lower than that of the bare film of B3PyMPM. These results suggest that the formation of an exciplex significantly retarded the carrier mobility of the co-host system. Because the carrier mobility was low and balanced in the exciplex co-host system, an extremely low efficiency roll-off of the device of BCzPh-pimi and BCzPh-mimi at high luminance was achieved. On the other hand, the low efficiency roll-off of the devices can also be explained by the architecture of the device. There are three layers capable of hole-transport and only one layer capable of electron-transport for the devices in this work. Consequently, hole-transport is faster than electron-transport in the device of BCzPh, which lowers the recombination efficiency of the charge carriers in the EML at a high driving voltage. Because the hole mobilities of BCzPh-pimi and BCzPh-mimi are lower than that of BCzPh, the recombination efficiency of holes and electrons was optimized in the corresponding devices. Compared to other reported green OLEDs with a low efficiency roll-off (Table 4), the BCzPh-pimi-based device in this work demonstrated the lowest efficiency roll-off of EQE, *i.e.*, 0.67%, at 10 000 cd cm^{-2} without a significant change in the electroluminescence spectra of the phosphorescent emitters. To the best of our knowledge, this is

Table 4 Summary of the representative green OLEDs with a low efficiency roll-off[a]

		Roll-off of EQE (%)				
EML (ref.)	Host (or emitter only)	Minimum	1000 cd m^{-2}	10 000 cd m^{-2}	EQE $_{max}$ (%)	CIE[x,y]
Exciplex host (this work)	BCzPh-pimi/B3PyMPM	0.67	2.73	0.67	22.31	(0.30, 0.64)
Exciplex host (this work)	BCzPh-mimi/B3PyMPM	1.44	1.44	6.19	18.73	(0.29, 0.64)
Exciplex host (this work)	BCzPh/B3PyMPM	3.24	3.24	6.61	25.54	(0.34, 0.62)
Exciplex host[16]	TAPC/TmPyPB	1.34	4.19	38.25	14.90	(0.34, 0.56)
Exciplex host[17]	mCP/DpTrz-BphBzAc	4.08	4.08	4.08	14.70	n.r.
Exciplex host[18]	BCzPh/3P-T2T	8.08	n.r.	8.08	29.70	n.r.
Exciplex host[19]	PhCzp-Me/B3PyMPM	2.83	2.83	9.59	27.84	(0.33, 0.62)
Exciplex host[25]	CzTrz/tBuTCTA	1.81	1.81	7.87	16.50	(0.32, 0.59)
Exciplex host[26]	TPAF/B3PyMPM	2.98	2.98	n.r.	20.10	(0.34, 0.63)
Exciplex host[27]	dCzPSi/PO-T2T	4.73	4.73	n.r.	21.10	(0.21, 0.49)
Ultrathin emitter[28]	Ir(ppy)$_2$(acac), emitter only	1.56	n.r.	4.70	24.30	n.r.
AIE emitter only[29]	TPB-AC, AIE emitter only	7.14	7.14	n.r.	21.00	(0.33, 0.63)
TADF host[30]	Sy	7.91	7.91	n.r.	24.00	(0.28, 0.55)

[a] n.r. = not reported.

the first example demonstrating a phosphorescent OLED with an efficiency roll-off lower than 1% at 10 000 cd cm^{-2} when its EQE is larger than 20%.

Conclusions

In summary, we synthesized two new BCzPh analogs, *i.e.*, BCzPh-pimi and BCzPh-mimi, by introducing a benzimidazole moiety to the *para*- and *meta*-positions of the phenyl ring of BCzPh. These molecules were blended with B3PyMPM to form an exciplex co-host system for OLEDs using $Ir(ppy)_2(acac)$ as the green phosphorescent emitter. The maximum EQE of the device of BCzPh-pimi reached 22.31%, suggesting an efficient charge transfer from the exciplex co-host to the emitter. Impressively, the device with BCzPh-pimi retained its EQE at 22.16% at a luminance of 10 000 cd cm^{-2}, corresponding to an extremely low efficiency roll-off of 0.67% only. Photophysical and carrier mobility analyses of the molecules reveal that BCzPh-pimi possesses a more effective π-conjugation length and lower hole mobility than BCzPh, suggesting that the optoelectronic properties of BCzPh could be adjusted by introducing a benzimidazole moiety to the *para*-position of the phenyl ring. The extremely low efficiency roll-offs of OLEDs can be attributed to the reduced hole mobilities of the donors in the exciplex co-host system, which optimized the balance in charge recombination in the EML of OLEDs. Our results provide a novel approach towards the development of a highly efficient OLED with an extremely low efficiency roll-off at high luminance for potential lighting applications.

Conflicts of interest

There are no conflicts to declare.

Acknowledgements

The authors acknowledge financial support from the Ministry of Science and Technology, Taiwan (Grant No. MOST 110-2221-E-131-019, 109-2223-E-131-001-MY3, 109-2113-M-032-002, and 110-2113-M-032-003). Also, the corresponding author (S.-W. Liu) is grateful to Mr H.-H. Wu, Syskey Technology Corporation (Taiwan), for his assistance in designing the fabrication system.

References

1 H. Uoyama, K. Goushi, K. Shizu, H. Nomura and C. Adachi, *Nature*, 2012, **492**, 234–238.
2 K. Goushi, K. Yoshida, K. Sato and C. Adachi, *Nat. Photonics*, 2012, **6**, 253–258.
3 T. Zhang, B. Zhao, B. Chu, W. Li, Z. Su, X. Yan, C. Liu, H. Wu, Y. Gao, F. Jin and F. Hou, *Sci. Rep.*, 2015, **5**, 10234.
4 N. R. A. Amin, K. K. Kesavan, S. Biring, C.-C. Lee, T.-H. Yeh, T.-Y. Ko, S.-W. Liu and K.-T. Wong, *ACS Appl. Electron. Mater.*, 2020, **2**, 1011–1019.
5 F.-M. Hsu, C.-H. Chien, C.-F. Shu, C.-H. Lai, C.-C. Hsieh, K.-W. Wang and P.-T. Chou, *Adv. Funct. Mater.*, 2010, **19**, 2834–2843.
6 S. Jhulki, S. Seth, A. Ghosh, T. J. Chow and J. N. Moorthy, *ACS Appl. Mater. Interfaces*, 2016, **8**, 1527–1535.
7 Y. Tao, Q. Wang, L. Ao, C. Zhong, J. Qin, C. Yang and D. Ma, *J. Mater. Chem.*, 2010, **20**, 1759–1765.
8 J. Zhao, X. Du, S. Yuan, C. Zheng, H. Lin and S. Tao, *Org. Electron.*, 2017, **43**, 136–141.
9 H. Lim, H. Shin, K.-H. Kim, S.-J. Yoo, J.-S. Huh and J.-J. Kim, *ACS Appl. Mater. Interfaces*, 2017, **9**, 37883–37887.
10 Y.-S. Park, W.-I. Jeong and J.-J. Kim, *J. Appl. Phys.*, 2011, **110**, 124519.
11 Y.-S. Park, S. Lee, K.-H. Kim, S.-Y. Kim, J.-H. Lee and J.-J. Kim, *Adv. Funct. Mater.*, 2013, **23**, 4914–4920.
12 Z. Wang, C. Wang, H. Zhang, Z. Liu, B. Zhao and W. Li, *Org. Electron.*, 2019, **66**, 227–241.
13 S. Yi, J.-H. Kim, Y.-J. Cho, J. Lee, T.-S. Choi, D. W. Cho, C. Pac, W.-S. Han, H.-J. Son and S. O. Kang, *Inorg. Chem.*, 2016, **55**, 3324–3331.
14 H. Shin, J.-H. Lee, C.-K. Moon, J.-S. Huh, B. Sim and J.-J. Kim, *Adv. Mater.*, 2016, **28**, 4758–4925.
15 S. Yuan, X. Du, J. Zhao, W. Liu, H. Lin, C. Zheng, S. Tao and X. Zhang, *Org. Electron.*, 2016, **39**, 10–15.
16 X. Lin, Y. Zhu, B. Zhang, X. Zhao, B. Yao, Y. Cheng, Z. Li, Y. Qu and Z. Xie, *ACS Appl. Mater. Interfaces*, 2018, **10**, 47–52.
17 M. Chen, J. Yang, Z. Ye, S. Wang, Z. Tang, G. Chen, Y. Zheng, Y. Shi, B. Wei and W.-Y. Wong, *J. Mater. Chem. C*, 2018, **6**, 9713–9722.
18 C.-J. Shih, C.-C. Lee, T.-H. Yeh, S. Biring, K. K. Kesavan, N. R. A. Amin, M.-H. Chen, W.-C. Tang, S.-W. Liu and K.-T. Wong, *ACS Appl. Mater. Interfaces*, 2018, **10**, 24090–24098.
19 C.-C. Lee, N. R. A. Amin, J.-J. Xu, B.-C. Wang, D. Luo, K. Sutanto, S. Biring, S.-W. Liu and C.-H. Chen, *J. Mater. Chem. C*, 2021, **9**, 9453–9464.
20 C.-J. Zheng, J. Ye, M.-F. Lo, M.-K. Fung, X.-M. Ou, X.-H. Zhang and C.-S. Lee, *Chem. Mater.*, 2012, **24**, 643–650.
21 D. Secci, A. Bolasco, M. D'Ascenzio, F. D. Sala, M. Yáñez and S. Carradori, *J. Heterocycl. Chem.*, 2012, **49**, 1187–1195.
22 H.-T. Mao, C.-X. Zang, G.-G. Shan, H.-Z. Sun, W.-F. Xie and Z.-M. Su, *Inorg. Chem.*, 2017, **56**, 9979–9987.
23 L.-S. Cui, Y. Liu, X.-D. Yuan, Q. Li, Z.-Q. Jiang and L.-S. Liao, *J. Mater. Chem. C*, 2013, **1**, 8177–8185.
24 W. Li, Y. Pan, L. Yao, H. Liu, S. Zhang, C. Wang, F. Shen, P. Lu, B. Yang and Y. Ma, *Adv. Opt. Mater.*, 2014, **2**, 892–901.
25 X. Song, D. Zhang, H. Li, M. Cai, T. Huang and L. Duan, *ACS Appl. Mater. Interfaces*, 2019, **11**, 22595–22602.
26 J. Zhao, X. Du, S. Yuan, C. Zheng, H. Lin and S. Tao, *Org. Electron.*, 2017, **43**, 136–141.
27 Y.-T. Hung, Z.-Y. Chen, W.-Y. Hung, D.-G. Chen and K.-T. Wong, *ACS Appl. Mater. Interfaces*, 2018, **10**, 34435–34442.
28 T. Zhang, C. Shi, C. Zhao, Z. Wu, J. Chen, Z. Xie and D. Ma, *ACS Appl. Mater. Interfaces*, 2018, **10**, 8148–8154.
29 Z. Xu, J. Gu, X. Qiao, A. Qin, B. Z. Tang and D. Ma, *ACS Photonics*, 2019, **6**, 767–778.
30 S.-W. Li, C.-H. Yu, C.-L. Ko, T. Chatterjee, W.-Y. Hung and K.-T. Wong, *ACS Appl. Mater. Interfaces*, 2018, **10**, 12930–12936.

